



## Investigation of the multiple-component structure of the 20 January 2005 cosmic ray ground level enhancement

K. G. McCracken,<sup>1</sup> H. Moraal,<sup>2</sup> and P. H. Stoker<sup>2</sup>

Received 20 September 2007; revised 21 August 2008; accepted 2 September 2008; published 5 December 2008.

[1] Worldwide observations of the cosmic ray ground level enhancement (GLE) of 20 January 2005 are used to investigate a commonly observed but poorly understood feature of this class of event. It is argued that the GLE comprised two distinctly different cosmic ray populations. The first resulted in an impulsive, highly anisotropic, field-aligned pulse with a relatively hard rigidity spectrum and significant velocity dispersion. The characteristics of the anisotropy were almost identical to those for similar impulsive increases observed during GLEs in 1960, 1978, and 1989. The  $\pi^0$   $\gamma$  ray observations from the RHESSI and CORONAS-F spacecraft and Type III radio emissions yield a path length of  $1.76 \pm 0.1$  AU to Earth for the first pulse. After the highest energies in the initial anisotropic pulse had passed Earth, another field-aligned but mildly anisotropic cosmic ray pulse developed slowly worldwide, exhibiting the characteristics of the conventional GLE. The risetime and anisotropy of this second population indicate substantial scattering, apparently at variance to the essentially scatter-free nature of the initial pulse. We show that the coexisting scatter-free initial impulsive increase and the diffusive character of the second pulse are consistent with the standard quasi-linear theory of pitch angle diffusion. Throughout the GLE, the anisotropy remained field-aligned, and a third maximum, seen by some stations, is shown to be due to changes in the direction of the heliospheric magnetic field (HMF). Examination of 22 large (>20%) GLEs in the historical record shows that the impulsive pulse never occurs after the commencement of the P2 pulse, indicating that the impulsive-gradual combination is not due to a chance sampling of differing scattering regions of the HMF. It is further shown that impulsive pulses, or their equivalents, have been observed in 13 out of the 15 GLEs associated with solar activity in the solar longitude range  $24^\circ$ – $98^\circ$ W, leading us to propose that the event of 20 January 2005 should be regarded as the defining example of the GLE. The observations lead us to propose two separate acceleration episodes in the typical GLE: (1) acceleration directly associated with the flare itself and located in the lower corona and (2) acceleration by a supercritical shock driven by the associated coronal mass ejection, located at  $\sim 3$ – $5$  solar radii and farther in the upper corona. A one-to-one association with so-called impulsive and gradual solar energetic particle events at lower energies is proposed. On the basis of these observations, a generic model for the GLE is proposed.

**Citation:** McCracken, K. G., H. Moraal, and P. H. Stoker (2008), Investigation of the multiple-component structure of the 20 January 2005 cosmic ray ground level enhancement, *J. Geophys. Res.*, *113*, A12101, doi:10.1029/2007JA012829.

### 1. Introduction

[2] The ground level enhancement (GLE) as seen by cosmic ray detectors on the surface of Earth is one of the most studied features of the cosmic radiation in the rigidity range 1–10 GV. It is generally understood to be due to a short-lived episode of cosmic ray acceleration, triggered by, or associated with a solar flare. This paper will show that

the nature of the GLE is more complex than usually thought and propose that it consists of two separate but closely associated phases, yielding strikingly different cosmic ray events at Earth. It is demonstrated that many past GLEs have been a combination of both phases in varying measure, which has disguised the true nature of the process occurring at the Sun, and introduced misconceptions regarding the scattering processes between the Sun and Earth.

[3] The earliest GLEs were observed with five Carnegie ionization chambers, and were usually reported in hourly, and occasionally in 15-min, integration intervals [Forbush, 1946]. It showed a rapidly rising intensity with a time scale of 0.25 to 1 h, followed by a monotonic decay with time scale of 6 to 24 h, with the amplitude varying substantially worldwide. The large event of 23 February 1956 was

<sup>1</sup>Institute for Physical Science and Technology, University of Maryland, College Park, Maryland, USA.

<sup>2</sup>School of Physical and Chemical Sciences, North-West University, Potchefstroom, South Africa.

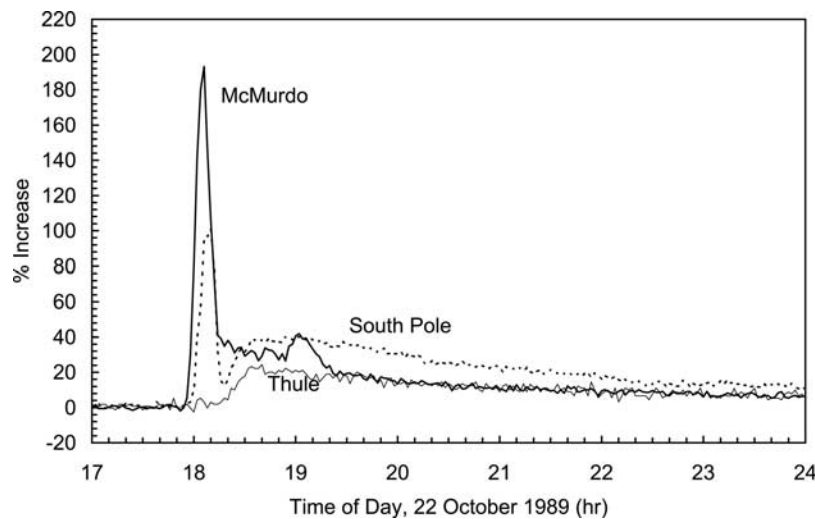


**Figure 1.** An example of an anomalous impulsive increase at the onset of the GLE of 22 October 1989 (after *Shea and Smart* [1996] with permission from American Institute of Physics). The impulsive increase was only seen by McMurdo, South Pole, Calgary, and Magadan. The GLE observed by more than 20 other neutron monitors was similar to the increase seen by Thule.

observed by many more detectors, including the first neutron monitors, and more features of the GLE phenomenon became apparent. The occurrence of “impact zones” was recognized, indicating that the radiation was initially anisotropic [*Firor*, 1954]. The onset times on stations dispersed around the world differed by up to 10 min. The decay was well described by a diffusion process when a reflecting boundary was assumed at  $\sim 1.5$  AU [*Meyer et al.*, 1956]. The diffusion model was further reinforced by the observation that the decay of the GLEs known at that time varied strongly from event to event, the decay time constant being much shorter when the parent flare was on the western portion of the solar disk [*McCracken and Palmeira*, 1960].

[4] Using the concept of asymptotic cones of acceptance, computed using a sixth-order expansion of the geomagnetic field, *McCracken* [1962a, 1962b] showed that several GLEs were strongly anisotropic when the parent flare occurred on the western third of the solar disk. In those cases, the anisotropic radiation arrived at Earth from a direction some  $50^\circ$ W of the Earth-Sun line, in good agreement with the prediction of the spiral nature of the HMF by *Parker* [1958]. For the very short-lived GLE of 4 May 1960 the intensity rose rapidly to a maximum, and the rigidity spectrum was relatively hard. Within the poor time resolution and poor statistics available from many of the detectors (0.25 or 1 h), *McCracken* showed that the initial anisotropy decayed over a period of  $\sim 1$  h. He also showed that for a parent flare on the eastern two-thirds of the solar disk the risetime of the GLE was considerably slower, the radiation was only mildly anisotropic ( $<20\%$ ), and the rigidity spectrum was relatively soft.

[5] On the basis of these observations, the present-day model of the GLE was largely complete. The model states that cosmic rays generated on the western third of the solar disk travel to Earth rapidly along the Parker spiral magnetic field, while experiencing both pitch angle scattering and adiabatic focusing, and arrive at Earth as an anisotropic beam from the prevailing direction of the HMF. Irregular-

ities and Alfvén waves in the HMF continue to scatter the cosmic rays so that they attain isotropy some 0.5 to 2 h later. In the case of production near the central solar meridian, there is no direct access, and the cosmic rays only reach Earth after diffusing across the HMF. As a consequence, the intensity rises more slowly to a maximum, it is only mildly anisotropic, the higher rigidities have largely left the inner solar system, and the radiation reaching Earth has a soft rigidity spectrum.

[6] The larger NM64 neutron monitors, developed in the 1960s, and the use of higher-resolution data acquisition systems led to the recognition that occasionally a GLE originating near the western limb of the Sun was extremely short-lived. This was most clearly demonstrated by the GLE of 4 May 1960 [*McCracken*, 1962b] and 7 May 1978 [*Shea and Smart*, 1982]. In both cases the rigidity spectra were harder than for the typical longer-lived GLE, and the intensity was extremely anisotropic. It was assumed that these were the limiting cases of a continuum of time scales, as a result of the scattering properties of the HMF varying over a rather large range. Later, *Shea and Smart* [1996] drew attention to the fact that occasionally one or two, out of say 30 neutron monitors, would see a rapidly rising and falling, short-lived precursor spike prior to the commencement of a conventional GLE at many more neutron monitors, an example being shown in Figure 1 for the GLE of 22 October 1989. They recognized that the spike was due to an extremely strong anisotropy, indicating little scattering, while the same event observed at other stations in the worldwide network was much less anisotropic, indicating relatively strong scattering. They issued a challenge for others to explain the coexistence of this weak and strong scattering, something that has remained unanswered to this day. Similarly, *Lovell et al.* [1998] showed that two separate pulses were observed for the lower rigidities in the GLE of 29 September 1989, while only the first (short-lived and highly anisotropic) pulse was seen at  $\geq 6$ GV. The community has regarded these precursor events as being due to a fortuitous magnetic connection of the Earth to the Sun,

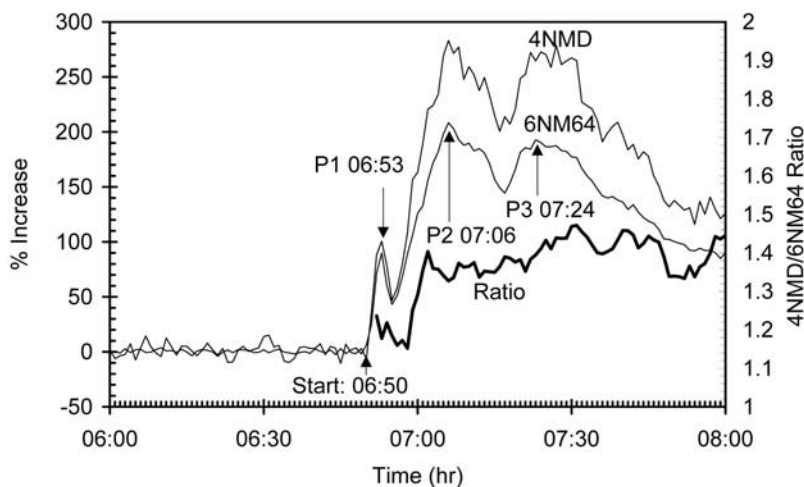


**Figure 2.** The GLE of 20 January 2005 as observed by the 6NM64 neutron monitor and the 4NMD neutron moderated detector (bare neutron monitor, without lead) at Sanae, Antarctica. The 4NMD/6NM64 ratio is shown by the thick line. The positions of the three peaks (as seen on the 6NM64) are marked as P1, P2, and P3.

without any impact on the prevailing model of the GLE. Two separate acceleration mechanisms have been proposed to explain the worldwide differences in GLE onset times [Shea and Smart, 1998], and spectral properties [Miroshnichenko et al., 2005; Bombardieri et al., 2006], however this postulate has not been widely accepted to date.

[7] There is a large body of experimental and theoretical studies of low-energy (<100 MeV) solar cosmic rays observed by satellites [e.g., Reames, 1999]. These studies have shown that there are two distinct classes of events, the impulsive and the gradual solar energetic particle (SEP) event. The impulsive events occur very frequently (>1000/yr) in close association in time with solar flares, and the isotopic composition (particularly the  $^3\text{He}/^4\text{He}$  and Fe/O ratios), ionization state, and other evidence indicates that they are due to cosmic rays accelerated in hot plasma in close proximity to the solar flare low in the corona. Their frequent association with quite small flares and interplanetary type III radio bursts has led to the conclusion that acceleration occurs in close proximity to open magnetic field [Reames, 2002, and references therein]. As a consequence, while some of the accelerated particles may be trapped in the closed sunspot fields, others leave the Sun immediately along the open field lines without hindrance or delay.

[8] The properties and associations of the gradual SEP events are quite different. They occur less frequently, and the evidence indicates that the particles are accelerated high in the corona (>4 solar radii), where the temperatures and densities are much lower. They are only observed in association with the relatively rarely observed high-speed coronal mass ejections (CME). Both the observations and theory indicate that the particles are accelerated in a supercritical shock being driven by the CME. To date, a clear correspondence between the GLE and these distinctly different classes of SEP events has not been established. In anticipation of this correspondence as a result of this paper, however, we call the initial pulse of the 20 January 2005 event impulsive, corresponding to the nomenclature of the SEP events.

[9] The GLE of 20 January 2005 was one of the largest GLE on record, and the high fluxes, together with a large number of neutron monitors with sharply defined asymptotic cones of acceptance, provide us with an unprecedented ability to study the nature of the impulsive spike and the more isotropic, subsequent gradual phase of this GLE. This we do with particular emphasis on the data from the Sanae neutron monitor, which was ideally placed to examine the characteristics of both these phases. We show that the impulsive phase has been observed frequently in the past for GLEs on the western portion of the solar disk. We use these results to establish the properties of both the impulsive and the more isotropic gradual phase of the event. Finally, we propose that these properties may require revision of the generic model regarding where the GLE particles are accelerated, and the manner of their propagation to Earth.

[10] Compared to previous large GLEs, there is a substantial body of data from satellite archives that has a major bearing on the analysis of this event. This paper uses the detailed measurements of the HMF, X-ray images and gamma ray intensity profiles of the parent solar flare as an integral part of the study. We also show that the historical record starting in 1942 provides key information that allows resolution of the ambiguities that arise when dealing with only one or two events.

## 2. Observations of the 20 January 2005 GLE

[11] Figure 2 presents the observations of the Sanae 6NM64 neutron monitor and the 4NMD neutron moderated detector (counters without lead) at  $71^{\circ}40'S$ ;  $02^{\circ}51'W$ , cutoff rigidity  $P_c = 0.79$  GV. The most striking feature is the presence of three distinct peaks. We will refer to them as P1, P2, and P3. The standard deviation on the one-minute data is 1% for the 6NM64, and 5% for the 4NMD, therefore the >100% peaks are highly significant.

[12] Figures 3 and 4 display the observations from a number of other neutron monitors in the worldwide network. Figure 5 gives the asymptotic directions of viewing

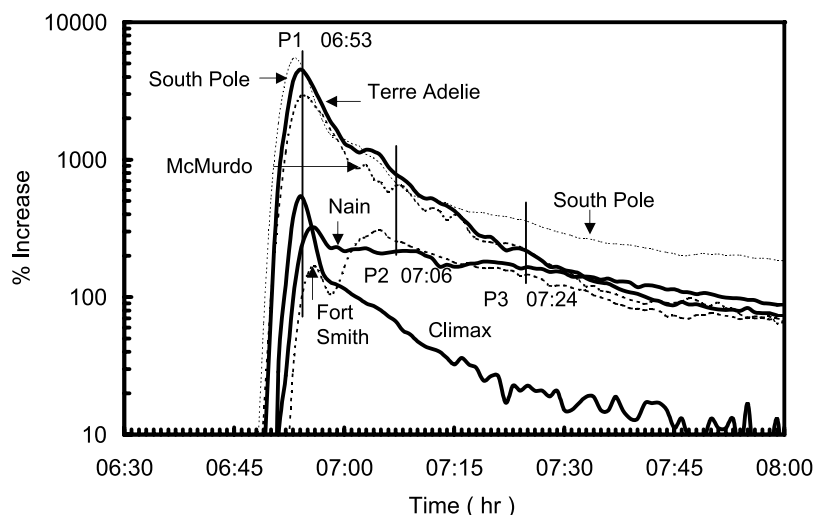


**Figure 3.** The GLE of 20 January 2005 observed by six other neutron monitors that distinctly observed pulse P1 as seen by Sanae. Vertical lines indicate the times of pulses P1, P2, and P3 as seen at Sanae.

for vertical incidence for these neutron monitors, computed by *Bombardieri* [2008], using the IGRF 2005 field model with external field components appropriate to  $K_p = 2$  and  $D_{st} = -58$ . The observations by the stations in Figures 3 and 4, as well as those from others not referenced here, show that the profiles and amplitudes of the GLE depended strongly on the asymptotic direction of viewing. Table 1 gives estimates of the onset times of the GLE in Figures 2, 3, and 4, and a difference of up to 8 min is evident. To examine this further, Figure 3 shows the data from the six neutron monitors that also saw the initial, impulsive increase, P1, seen by Sanae. Table 1 shows that they observed the earliest onset times and we conclude that all seven, as well as the GRAND muon and Milagro Cerenkov detectors (see section 5) saw the same pulse of radiation. Sanae, Climax and South Pole saw the earliest P1 increases, and the first fluxes arrived at  $\sim 0650$  UT. The P1 pulse at Sanae reached a peak at  $\sim 0653$  UT and the intensity then fell

rapidly to half the peak value in  $\sim 2$  min. Thereafter, the intensity started to increase in a monotonic manner for the next 8 min, reaching the maximum of P2 at  $\sim 0706$  UT, in good agreement with many other neutron monitors. The intensity then declined steadily until 0716 UT, whereafter it increased again, reaching a broad peak, P3, in the vicinity of 0724 UT.

[13] Next we discuss the hardness of the accelerated spectra. We first note that the spectra extended to quite high rigidities. The GRAND air shower array ( $P_c = 11$  GV) [*D'Andrea and Poirier*, 2005] and the Milagro gamma ray telescope ( $P_c > 4$  GV) [*Ryan and the Milagro Consortium*, 2005] saw the impulsive pulse P1 with amplitudes of  $\sim 13\%$  and  $\sim 12\%$ , respectively. Milagro also saw a recognizable gradual pulse P2. Furthermore, the Tibet neutron monitor ( $P_c = 14.1$  GV) saw a 1.7% increase coincident with P2 [*Miyasaka et al.*, 2005]. Next we note that both Sanae and South Pole obtained data with NM64 neutron monitors and

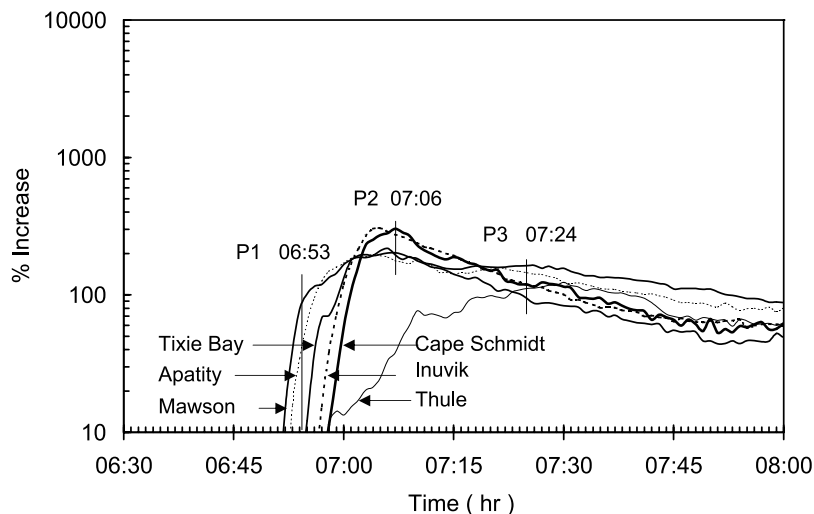


**Figure 4.** The GLE of 20 January 2005 observed by six other neutron monitors that did not distinctly see P1 as seen by Sanae. These monitors have narrow cones of acceptance. Vertical lines indicate the times of pulses P1, P2, and P3 as seen at Sanae.

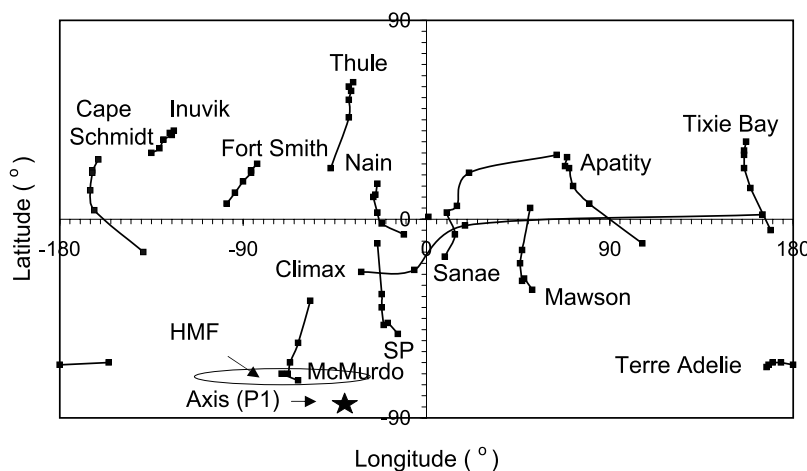


**Figure 5.** Asymptotic cones of acceptance in geographic coordinates for particles arriving vertically at the neutron monitors used in Figures 2, 3, and 4. Note the elongated nature of the Sanae and Climax cones. The six markers on each station's worm are for rigidities of 6, 5, 4, 3, 2, and 1 GV (Climax only down to 3 GV), with the highest rigidity nearest to the station name. The oval demarcates the range of directions of the heliospheric magnetic field (HMF) during the event (see Figure 7), while the star symbol shows the axis of symmetry of the cosmic ray anisotropy at the peak of pulse P1.

neutron moderated detectors (NMD), which are counters without lead producers. According to *Stoker* [1994] these NMDs are more sensitive to lower-energy particles, and consequently the NMD/NM64 ratio is sensitive to the spectral index of the GLE radiation. The thick line in Figure 2 shows that the 4NMD to 6NM64 ratio for Sanae had a low value of  $\approx 1.2$  throughout P1, while it increased rapidly during the transition from P1 to P2 to values between 1.4 and 1.5 up to a time well past P3, at 0730 UT. Thereafter it gradually hardened again to its ambient (interstellar) value. Using the methodology of *Stoker* [1994] and *Stoker et al.* [2000], this implies that for a power law in rigidity,  $P^\gamma$ , the spectral index was  $\gamma \approx 4-5$  for P1 and  $\gamma \approx 5-6$  during P2 and P3. (Allowance was made for the effects of the anisotropy - to be published). From similar measurements at South Pole, *Bieber et al.* [2005] observed the same softening with time, with  $\gamma \approx 3.75$  for P1, and  $\gamma \approx 4.75$  for P2. Using the more accurate global modeling methodology, *Bombardieri* [2008] and *Flueckiger et al.* [2005] obtained significantly higher values of  $\gamma$ . However, both concluded that  $\gamma$  increased by  $\sim 2$  between P1 and P2. *Miroshnichenko et al.* [2005] and *Bombardieri et al.* [2006] have previously shown that the spectrum softened for other GLEs with the passage of time, and they proposed that this was not entirely due to propagation effects but partly due to a harder production spectrum at the commencement of the event. Thus, taken together, these and other studies lead us to conclude that the rigidity spectrum of P1 was significantly harder than that of P2 and P3.

[14] Sanae was the only high-latitude neutron monitor that clearly observed all three pulses. It is unique among high-latitude neutron monitors because, although it has a low geomagnetic cutoff rigidity ( $P_c = 0.79$  GV), its asymptotic cone of acceptance is not narrow as is typical for such monitors, but wide as for high-cutoff, low-latitude monitors. This is shown in Figure 5. As a consequence, Sanae saw (1) the high-rigidity ( $\sim 5$  GV) particles coming from  $10^\circ$ S,  $15^\circ$ E, (2) intermediate (2–4 GV) particles from  $0^\circ$  to

$20^\circ$ N and  $10^\circ$  to  $20^\circ$ E, and (3) low-rigidity ( $<1.5$  GV) particles from  $\geq 40^\circ$ E.

[15] Figure 4 displays the data from neutron monitors that did not clearly see pulse P1. The character of the GLE at these stations was strikingly different from those in Figure 3. To fix ideas, consider Inuvik and Cape Schmidt, the stations that saw the latest onset times. The intensity started rising at both stations at  $\sim 0657$  UT, and rose steadily at about 10 to 15% per minute for the following 8 min, reaching the broad peak, P2, at  $\sim 0706$  UT. Thule started at the same time, but according to Figure 5 its asymptotic cone of acceptance was so far removed from the sunward direction of the HMF that the intensity did not reach a maximum until well after P2. Stations such as Apatity, Mawson, and Tixie Bay display onset times that are intermediate between the extremes. Mawson has a point of inflection on its rising phase, and

**Table 1.** Onset and Peak Times of the Pulses P1 and P2<sup>a</sup>

Station	GLE Start	P1 Max	P1 Amp (%)	P2 Max (UT)
South Pole	0649:45	0653:45	2180	–
McMurdo	0650:00	0655:30	2860	–
Terre Adelie	0650:15	0654:30	4527	–
Climax	0650:00	0653:00	542	–
Sanae	0650:00	0652:45	90	0706
Nain	0652:30	0655:45	220	0708
Fort Smith	0653:00	0656:00	150	0705
GRAND	0651:00	0653:00	12.9	–
Milagro	0651:00	0652:45	11.7	0702
Tixie Bay	0654:15	–	–	0706
Inuvik	0657:00	–	–	0705
Cape Schmidt	0658:00	–	–	0707
Apatity	0652:45	–	–	0705
Mawson	0651:45	–	–	0707

<sup>a</sup>Times are estimated to an accuracy of  $\pm 15$  s using the relative values of adjacent measurements. The top section lists the neutron monitors that clearly saw P1; the second section summarizes the muon observations; the third section gives neutron monitors that did not see P1, while the two in the bottom section are interpreted as having seen both, but not as separate pulses. The South Pole amplitude has been corrected to sea level using the two attenuation length method of *McCracken* [1962a].

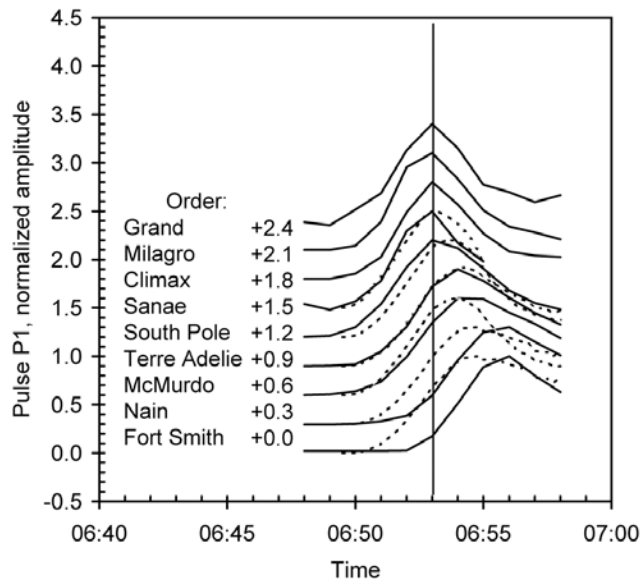


**Figure 6.** Illustrating the velocity dispersion inherent in pulse P1. Intensities are normalized to unity, with accumulative factors of 0.3 added to separate them. The vertical line marks the time of peak intensities at the earliest stations, 0653. The dashed lines are the calculated pulse shapes allowing for velocity dispersion as described in the text. The weighted mean pitch angles (relative to the anisotropy) of the lower four stations are  $28^\circ$ ,  $31^\circ$ ,  $80^\circ$ , and  $95^\circ$ .

we interpret this as the neutron monitor seeing a fraction of the intensity in pulse P1, partially merged with the commencement of P2. We note from Figures 3 and 4 and Table 1 that there is good agreement between the times of maxima, and the shape of the second pulse, P2, between all stations that saw it, other than Thule.

[16] To further study the nature of P1, Figure 6 displays the increases normalized to the peak intensities attained during that pulse. Given the fact that the Terre Adelie increase was  $\sim 40$  times larger than at Sanae and Fort Smith, there is remarkably good agreement between all seven neutron monitors and the high-energy detectors about the general features of the pulse shapes. The 1–3 min differences in onset time, time of maximum, and pulse duration, will be discussed and modeled in section 5.

[17] Referring back to Figure 2, there was a  $\sim 20\%$  decrease at  $\sim 0715$  UT in the intensity of pulse P2 that preceded a third pulse, P3. This third increase was also marginally seen by neutron monitors with asymptotic directions in the vicinity of  $60^\circ\text{E}$ , such as Apatity and Mawson (Figure 4). It reached a maximum at 0724 UT on the 6NM64 at Sanae. A similar but somewhat later peak was observed at Thule. These results will be discussed later when we have quantified the anisotropies in the cosmic radiation.

[18] In summary, the observations indicate that P1 was due to a highly anisotropic, short-lived pulse of cosmic rays that commenced at  $\sim 0650$  UT and was seen by a few neutron monitors. As it was decreasing from its peak, the majority of neutron monitors throughout the world began to

see a slowly increasing pulse that commenced abruptly at  $\sim 0658$  UT, resulting in P2. The nature of the anisotropy in these pulses is discussed in section 3.

### 3. Anisotropies in the Cosmic GLE Radiation

[19] As developed by McCracken [1962a] and enhanced and used by many others [e.g., *Shea and Smart*, 1982; *Cramp et al.*, 1997; *Lovell et al.*, 1998; *Bieber et al.*, 2002; *Flueckiger et al.*, 2005] the asymptotic directions of viewing of neutron monitors can be used to quantify the anisotropic nature of the cosmic radiation in space. Thus, the asymptotic direction of viewing,  $\mathbf{A}(P)$ , for rigidity  $P$ , is determined for each detector using a model for the geomagnetic field, and the observed intensities are associated with those directions. On the basis that the GLE intensity will be a function of the pitch angle with respect to the direction of the HMF vector,  $\mathbf{B}$ , the direction is then found that allows the observations to be fitted as a function of the angle between a station's mean asymptotic direction,  $\mathbf{A}$ , and the axis of symmetry,  $\mathbf{S}$ , for the observed data. The more recent applications of "global modeling," e.g., by *Shea and Smart* [1982], *Cramp et al.* [1997], and *Lovell et al.* [1998], have integrated the response over the asymptotic cone, allowing for the directional dependence of the cosmic radiation within the cone, to achieve the same end.

#### 3.1. Heliospheric Magnetic Field

[20] High-resolution measurements of the vector HMF were made throughout the GLE of 20 January 2005 by the Advanced Composition Explorer (ACE), situated  $1.4 \times 10^6$  km from Earth in the direction of the Sun. The field observed at ACE exhibited  $\sim 80^\circ$  excursions in longitude throughout the period in which the solar cosmic rays reached Earth. The solar wind speed was  $\sim 800$  km/s at the time of the GLE, suggesting that the magnetic field entrained in the wind would reach Earth  $\sim 29$  min after observation at ACE, as illustrated in Figure 7. We note, however, that the gyroradius of a 2 GV cosmic ray is comparable to the distance between ACE and the Earth, and consequently, a neutron monitor on Earth might sample solar cosmic radiation spiraling along field lines whose vector directions could differ by as much as  $80^\circ$  at any given time. As a result, an anisotropy in the solar cosmic radiation at Earth would not be necessarily aligned with the instantaneous direction of the HMF; it would be determined by the anisotropic flows integrated over a substantial volume of space. The bar in Figure 7 indicates the likely range of vector directions that will influence the solar cosmic rays observed at Earth at any given time. This indicates that the direction of the anisotropies at Earth would vary over the range  $20^\circ$ – $70^\circ$  west of the Sun-Earth line, in broad response to the time-varying vector directions given in Figure 7.

#### 3.2. Anisotropy in the Initial Pulse P1

[21] We have used a simplified version of the global modeling method to determine the axis of symmetry of the radiation at the peak of pulse P1 to be in the approximate direction  $85^\circ\text{S}$ ,  $40^\circ\text{W}$  as shown in Figure 5. For the purposes of this paper we deemed it sufficient to use the asymptotic directions for vertical incidence only, computed

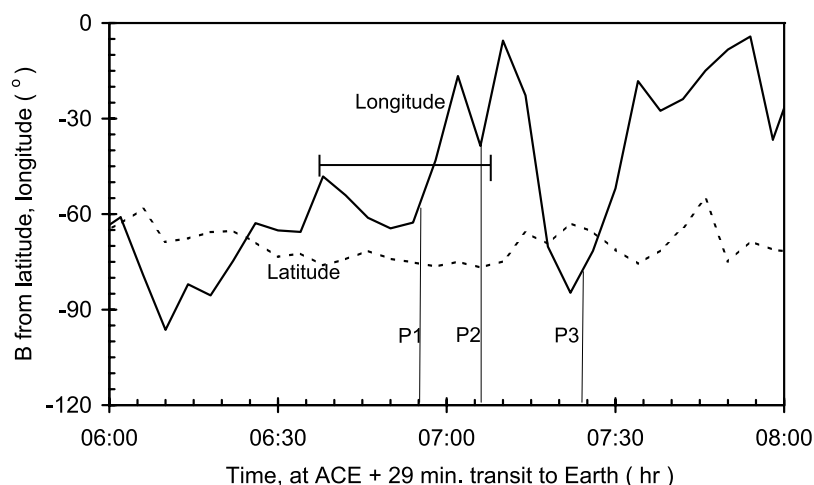


**Figure 7.** The heliospheric magnetic field as measured by the ACE spacecraft  $1.4 \times 10^6$  km in the sunward direction of Earth, transformed into the geographic coordinates. The time scale has been advanced by 29 min to allow for propagation to Earth at  $800 \text{ km s}^{-1}$ . The horizontal bar in the middle represents the time interval in which the distance of the gyroradius of a 2 GV particle ( $\sim 0.01$  AU) would pass a point of observation at this solar wind speed.

with the *Tsyganenko* [1989] field model, with IGRF 2005 parameters, and adjustments for the  $K_p$  and  $D_{st}$  indices provided by D.J. Bombardieri and M. Duldig. Further, the modeling was restricted to stations with asymptotic cones of limited angular extent, and the data were fitted to a Gaussian in pitch angle,  $\theta$ . Recognizing the presence of velocity dispersion in the data, we have chosen to model the peak values in the one-minute data displayed in Figure 3. Figure 8 displays the peak intensities plotted against the mean angle  $\theta$  between the mean asymptotic directions of viewing of each station (averaged over the observed anisotropy) and the axis of symmetry. The e-folding angle of the Gaussian curve through the points is  $\sim 50^\circ$ , which means that the radiation was highly anisotropic. The complete absence of P1 in the Tixie Bay, Cape Schmidt and Inuvik data indicates that there was no detectable radiation with pitch angles  $\theta \geq 100^\circ$ . Similar anisotropic distributions have been reported by *Plainaki et al.* [2007] and *Bombardieri* [2008].

[22] The GLEs of 4 May 1960 and 7 May 1978 were of similar duration to that of pulse P1 discussed here. The pitch angle distributions of those earlier GLEs are given by *McCracken* [1962b] and *Shea and Smart* [1982], and are reproduced in Figure 8. There is a remarkable similarity between these three pitch angle distributions. As noted in section 1, the rigidity spectra of these earlier GLEs were harder than those of most and, as noted in section 2, this is true for pulse P1 under discussion. The data for the P1 pulse of the GLE of 22 October 1989 (Figure 1) are consistent with these pitch angle distributions as well. That is, all four of these well-observed pulses had (1) short durations, (2) very similar pitch angle distributions, and (3) hard rigidity spectra. This leads us to postulate that they are all produced by similar mechanisms, despite the absence of the slower P2 pulse in the events of 4 May 1960 and 7 May 1978.

### 3.3. Anisotropy in the Second Pulse P2

[23] The axis of symmetry was determined to be approximately  $70^\circ\text{S}$ ,  $70^\circ\text{W}$  at the peak of P2 at 0706 UT, and also

at 0715 UT. By 0740 UT it had changed to approximately  $60^\circ\text{S}$ ,  $0^\circ\text{E}$ . Bearing in mind the averaging nature of the anisotropy as discussed in section 3.1, it is clear that the large westward excursion of the HMF between 0710 and 0722 UT (Figure 7) resulted in the  $\sim 30^\circ$  westward shift of the axis of symmetry noted between the peaks of P1 and P2. The subsequent eastward movement of the axis of symmetry is consistent with the large eastward excursion of the HMF between 0722 and 0754 UT (Figure 7). Thus, while the averaging nature of the anisotropy means that one cannot expect one-to-one correspondence between the field and the anisotropy direction, the general agreement noted above indicates that the anisotropy remained approximately field-aligned until after 0740 UT, despite the changing direction of the field.

[24] Figure 9 displays the dependence of the observed intensities upon the angle  $\theta$  between the mean asymptotic direction of viewing and the axis of symmetry for the three above times. It shows that there was a relatively weak dependence of intensity upon direction for  $\theta > 40^\circ$  at all three times. (The GRAND, Milagro and Climax observations indicate that P1 decreased to  $\sim 20\%$  of the peak value by 0658, and then more slowly until  $\sim 0715$ . This, together with velocity dispersion of the lower rigidities is the likely reason for the relatively high fluxes still observed by McMurdo at 0706, because it had a pitch angle of only  $15^\circ$ .) In particular, note that (1) the intensities only differed by  $< 25\%$  between  $\theta = 60^\circ$  and  $110^\circ$  at the peak of P2, (2) at all times the flow direction was outward along the HMF, and (3) there is no suggestion of an increase in “back-scattered” radiation from the antisolar direction after 0715 UT. In summary, there was a relatively weak, steadily decreasing anisotropy throughout pulse P2, whose direction of arrival changed by  $\sim 70^\circ$ , in response to the changes in the direction of the HMF at Earth. Unlike P1, there were substantial fluxes from pitch angles  $> 90^\circ$  from the initial onset of P2 at 0658 UT (as can be seen from the Inuvik and Cape Schmidt data in Table 1 and Figure 4).

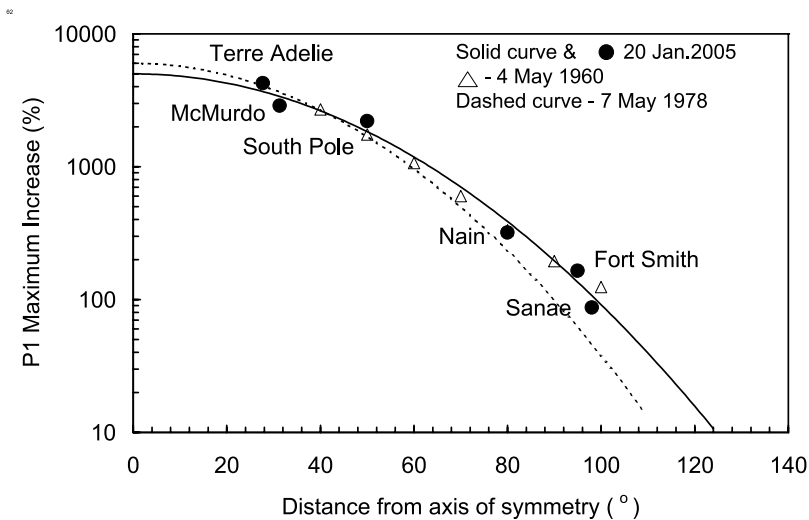


**Figure 8.** The anisotropic nature of pulse P1, based upon an axis of symmetry of 85°S, 40°W. Increases are shown in large dots. The increase at South Pole is corrected to its effective value at sea level. The solid curve through the points is the best fit Gaussian,  $5000 \exp[-(\theta/50.0)^2]$ , described in the text. The dashed curve is the anisotropy derived by *Shea and Smart* [1982] for the 7 May 1978 event, normalized to the size of this event by  $6000 \exp[-(\theta/41.7)^2]$ . The triangular symbols are the anisotropies for the 4 May 1960 event calculated by *McCracken* [1962b].

[25] The nature of pulse P2 was therefore greatly different from that of P1. The first pulse rose to a maximum very rapidly, and decayed almost as quickly. It was highly anisotropic with little flux at  $\theta > 90^\circ$  and no significant flux at  $\theta > 100^\circ$ . By way of complete contrast, P2 exhibited slower rise and fall times and mild anisotropic characteristics from its initial onset, similar to many GLEs in the past. Thus, pulse P2 has the characteristics usually associated with the “conventional” GLE, while P1 provides a clear example of the “spikes” occasionally resolved in past GLEs [McCracken, 1962b; *Shea and Smart*, 1996; *Cramp et al.*, 1997].

**3.4. Nature of the Third Pulse P3**

[26] To fix ideas, consider the anisotropy at 0715 UT in Figure 9. This implies that changes in the direction of the HMF will introduce increasing fluxes at some stations and decreases at others, depending on the consequent changes to the pitch angles reaching the station in question. Anisotropies such as in Figure 9 and pitch angle changes  $>20^\circ$  will introduce changes of 20 to 30% into the GLE time profile. This implies that changes in the vector HMF, such as shown in Figure 7, will introduce substantial differences into the detailed time profiles observed worldwide, in addition to the more obvious differences in event amplitude due to the different average pitch angles of viewing.

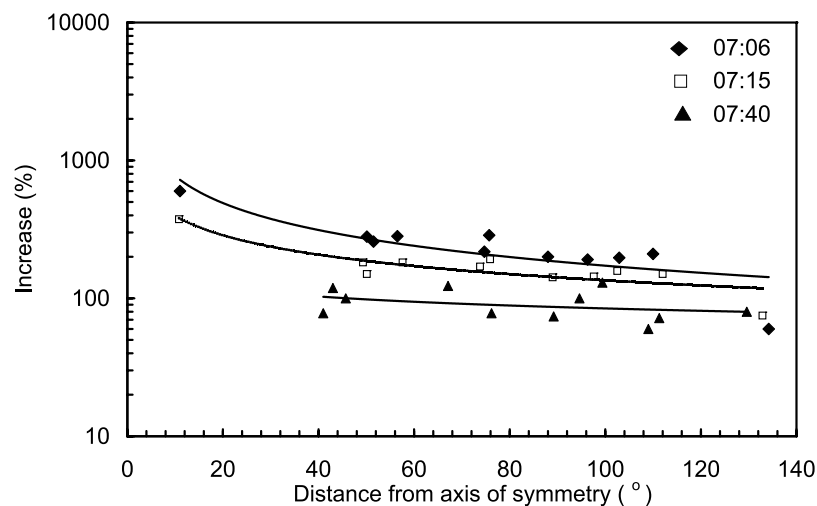


**Figure 9.** The anisotropic nature of the main phase of the event at 0706 UT (maximum of pulse P2), 0715 UT, and 0740 UT. The optimum axes of symmetry for these three times were (70°S, 70°W), (70°S, 70°W), and (60°S, 20°E).



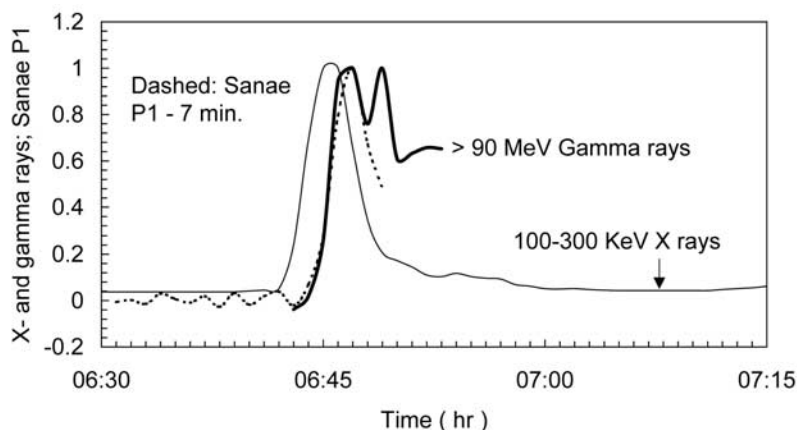


**Figure 10.** X-ray and  $\gamma$  ray emissions, observed by the RHESSI and CORONAS-F spacecraft, respectively, together with the P1 cosmic ray pulse observed by Sanae. This pulse is shifted backward in time by 7 min. The time scale is observation time at Earth. All profiles are normalized to their peak values. The CORONAS-F data are from *Kuznetsov et al.* [2007] and V. G. Kurt (private communication, 2007).

[27] Figure 2 shows that the intensity at Sanae exhibited a broad minimum in the vicinity of 0714 UT, followed by an increasing intensity to peak P3 at  $\sim$ 0724 UT. The same feature is shown to a lesser extent by Apatity and Mawson in Figure 4. For the purpose of this discussion we note that the asymptotic cones of all three neutron monitors (for  $<2$  GV particles) were in the longitude range  $30^{\circ}$ – $100^{\circ}$ E. The observed axis of symmetry was in the vicinity of  $70^{\circ}$ S,  $70^{\circ}$ W at 0715 UT, leading to the result that the 1 GV radiation was approaching the three stations from  $100^{\circ} < \theta < 130^{\circ}$ . Over the subsequent 10 min the axis of symmetry swung to the vicinity of  $60^{\circ}$ S,  $0^{\circ}$ W, with the result that  $75^{\circ} < \theta < 100^{\circ}$ . Similar changes in  $\theta$  applied for 2–4 GV cosmic rays. That is, the changing direction of the HMF caused the three stations to progressively sample smaller pitch angles between 0714 and 0724 UT. The anisotropy for 0715 UT in Figure 9 shows that this change in  $\theta$  would result in an  $\sim$ 20% increase in the cosmic ray intensity. This is in broad agreement with the increases observed at all three of the stations discussed above. Thus, we explain peak P3 in terms of the rotation of the field-aligned, anisotropic distribution of cosmic rays through their asymptotic cones of acceptance, as a consequence of the changing direction of the HMF.

#### 4. Solar Observations

[28] The GLE was associated with a GOES Class X7.9 solar flare that erupted at 0636 UT at  $14^{\circ}$ N and  $67^{\circ}$ W on the Sun. Table 2 summarizes the associated electromagnetic phenomena, while Figure 10 displays the hard X-ray (HXR) and gamma ray emissions observed by the RHESSI and CORONAS-F spacecraft. Both Table 2 and Figure 10 show that an intense burst of hard X rays commenced rapidly at  $\sim$ 0643 UT, followed by a rapidly increasing flux of  $>90$  MeV gamma rays  $\sim$ 0645 UT. The rising phases of these emissions, and other gamma ray observations from 17 MeV upward, were very similar. The HXR pulse indicates that a large population of relativistic electrons was accelerated during the  $\sim$ 2 min starting at 0635 solar

time (ST) (allowing for a photon transit time of 500s). The  $>90$  MeV gammas originate in the decay of  $\pi^0$ -mesons [*Grechnev et al.*, 2008] produced by the interaction of  $>300$  MeV cosmic rays with solar matter. Figure 10 therefore shows that a large population of cosmic rays attained relativistic energies between 0637:10 and 0638:20 ST. The  $>60$  MeV CORONAS-F data of *Grechnev et al.* [2008] show a smaller (5%) gamma ray burst, commencing at 0643:45 UT, indicating that a small population of cosmic rays may have been generated in close association with the beginning of the HXR event, followed by the main cosmic ray acceleration process about one minute later.

[29] We now discuss the context in which these relativistic populations were accelerated.  $H_{\alpha}$  ribbons were first observed at 0640:47 UT in areas of exceptionally strong magnetic fields, as described by *Grechnev et al.* [2008], and maximum  $H_{\alpha}$  emission occurred  $\sim$ 0647:30 UT. Type III radio emissions commenced at  $\sim$ 0645 above 300 MHz, descending rapidly in frequency over the next minute to  $<10$  MHz, indicating the escape of fast electrons into interplanetary space via open field lines. The RHESSI spacecraft carried an imaging spectrometer that allows us to understand the spatial and temporal features of the electron acceleration process. To this end, Figure 11 displays selected images of the solar event in the energy ranges 12–25 KeV and 100–300 KeV. The full sequence of these images can be examined at <http://www.astro.phys.ethz.ch/staff/shilaire/hessi/daily.1c/>. (There are no images at higher photon energies.) The images of Figure 11 and the time profiles in Figure 10 reveal the following time sequence.

[30] The 12–25 KeV SXR flux started to increase slowly at 0634 UT, and then rose much more sharply from 0643 UT onward, to reach a broad maximum at 0649 UT, and fell relatively slowly thereafter. The top two rows of images in Figure 11 for this energy show that the emitting region was initially centered at about  $14^{\circ}$ N and  $65^{\circ}$ W. Up until 0639 UT all of the SXR emission was centered on  $65^{\circ}$ W, with very little emission near  $60^{\circ}$ W. At 0639 UT the SXR bright emission region at  $65^{\circ}$ W started to extend in a loop-like structure that terminated in two bright spots in the vicinity

**Table 2.** Summary of the Electromagnetic Emissions From the Flare Associated With the GLE of 20 January 2005<sup>a</sup>

Observation (UT)	Start Time (UT)	Maximum
H $\alpha$ emission	0640:47 (1)	0647:30 (1)
Radio - 80 GHz	0643:15 (1)	0647:00 (1)
Radio - Type III	0645:06:46 (2)	0650 (2)
Soft X rays	0634/06:43 (3)	0649:00 (3)
Hard X rays	0643:00 (3)	0645:30 (3)
$\pi^0$ gamma rays	0645:30 (4)	0646:30 (4)

<sup>a</sup>Sources: 1, *Grechnev et al.* [2008]; (2) H. Cane and W. Ericson (private communication, 2007); 3, RHESSI data; 4, V. G. Kurt (private communication, 2007). Further details are given in the text.

of 60°W. In the subsequent three minutes these bright spots intensified greatly, becoming consolidated at 12°N, 58°W, and 15°N, 60°W. The presence of the loop-like emission image and the two bright spots 7° east of the initial emissions leads us to the view that the SXR emissions were initially from hot plasma at a considerable height in the corona ( $\sim 0.2 R_s$ ), and that at  $\sim 0639$  UT the emitting region extended down the magnetic field lines to the vicinity of the chromosphere, with H $\alpha$  emission being observed soon after, at 0640:47 UT. The field-aligned nature of the SXR emissions indicates that they were due to charged particles interacting with coronal magnetic fields and gas nuclei. The loop-like nature of the image and the bright spots remained intact until after 0651 UT.

[31] The behavior at higher photon energies and in the radio spectrum was distinctly different. For example, there

was relatively little change in the 100–300 KeV flux until  $\sim 0643$  UT, when it rose rapidly to a sharp peak at  $\sim 0645:30$  UT, and then fell almost as rapidly, attaining its 50% intensity by  $\sim 0647:30$  UT. The images in Figure 11 reveal that the short-lived pulse of HXR originated some 5° to 7° to the east of the initial source of the SXR, and were primarily from the two intense emitting regions evident in the SXR image, each of angular extent  $< 2^\circ$  in solar coordinates. The evidence summarized above suggests that these were the mirror points of a population of trapped relativistic electrons.

[32] As discussed above, the  $>90$  MeV gamma ray pulse shows that cosmic rays attained relativistic energies soon after the relativistic electrons. The near-coincidence in time suggests that there was a close association between the acceleration of the relativistic electrons and ions, and that the  $\pi^0$ -mesons responsible for the  $>90$  MeV gamma rays were probably generated in the vicinity of the intense emitting regions in Figure 11. That is, we propose that the relativistic electrons generated X-ray bremsstrahlung, while the cosmic rays produced  $\pi^0$ -mesons in the higher coronal mass densities near the mirror points of the sunspot magnetic fields, starting at 0637:10 ST. The Type III radio emissions indicate that electrons were escaping on open field lines by 0638 ST. In section 5 we investigate the consequences of the hypothesis that a burst of cosmic rays escaped into the open field coincident with the electrons responsible for the Type III radio emissions.

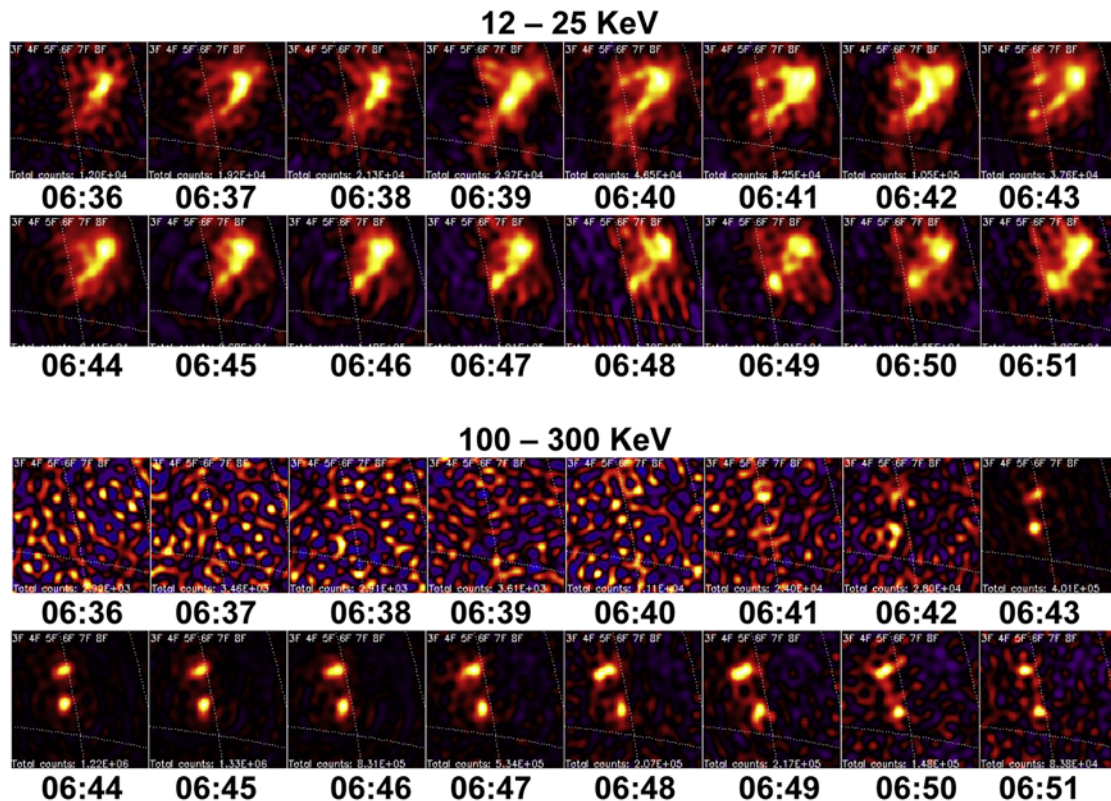


**Figure 11.** X-ray images from the vicinity of the flare. Times are observation time at Earth. The speckled nature of the 100–300 KeV image is due to detector noise, which is suppressed by the strong  $\gamma$  ray flux commencing at 0643 UT.

[33] The highly anisotropic nature of the prompt P1 pulse, compared to the relative isotropy of P2, may provide an important insight into the source of P1. In section 7.1 we show that it is consistent with the diffusive properties of the HMF if the P1 cosmic rays have been injected onto open field lines low in the corona (as were the Type III electrons), while the mild anisotropy of P2 is consistent with it being released into the open field at a height of  $\sim 3.3\text{--}3.8$  solar radii.

## 5. Velocity Dispersion Effects in Pulse P1

[34] The solid lines in Figure 6 display the normalized P1 pulses observed by the seven neutron monitors that saw P1, and by the GRAND and Milagro high-energy detectors. The top four time profiles are essentially identical. Examination of the asymptotic cones of all four detectors (two are given in Figure 5), and the anisotropy displayed in Figure 8, indicates that they were all observing  $>3$  GV cosmic rays. That is, the top four detections systems were seeing the same pulse of high-rigidity cosmic rays, all traveling at essentially the same speed, with  $\beta = v/c > 0.95$ .

[35] The rising phases in Figure 6 were all similar up to their peaks, but the lower four were increasingly delayed in time, by up to 3 min for Nain. Further, the nature of the decay phase became increasingly drawn out toward the bottom of the diagram. The rapid risetimes, and the overall similarity to the rapid rise of the  $>90$  MeV gamma ray pulse in Figure 10 suggests that a portion of the newly accelerated solar cosmic ray population was injected onto open HMF lines along with electrons (responsible for the Type III), and propagated to Earth with little scattering.

[36] To test this hypothesis we have modeled the arrival at Earth of a burst of cosmic radiation that left the Sun with a spectrum given by  $J(P, t) = P^{-\gamma} A(t-t_p/\beta)$ , where  $\gamma$  is the spectral exponent, and the pulse shape at the Sun,  $A(t)$ , is an isosceles triangle of base length 6 min, and  $t_p$  is the time of flight to Earth for the highest-rigidity particles. We then approximated the GLE enhancement at the  $n$ th station by

$$N_n(t) = \int_{P_l}^{\infty} S(P) G_n(\theta) J(P, t) dP, \quad (1)$$

where  $S(P)$  is the specific yield function as given by *Clem and Dorman* [2000], and  $G_n(\theta)$  is the pitch angle dependence from Figure 8 for the  $n$ th station. Anticipating a later result,  $t_p = 900$  s. We have varied the lower limit,  $P_l$ , to determine the contribution of higher-rigidity particles to the pulse at Earth. The dotted lines in Figure 6 present the computed pulses, and show that the velocity dispersion predicts the main features of the observed delay, and the slower decay of the pulses at the bottom of the figure. From this we conclude that (1) the initial portion of the rising phases are coincident at Terre Adelie, South Pole; McMurdo, Sanae and Climax because they are all due to the high-energy ( $>3$  GV) portion of the cosmic ray spectrum; (2) Nain and Fort Smith have little ( $<15\%$ ) response to the high-rigidity portion of the spectrum (see Figure 5), and consequently they exhibit an onset delay of  $\sim 2.5$  min due to velocity dispersion; and (3) while Sanae

and Climax only see the high-energy portion of the spectrum, Terre Adelie, South Pole and McMurdo see the low rigidities as well, thereby increasing the duration of P1 as the lower-rigidity components of the spectrum arrive. Figure 6 shows that the observations at Nain and Fort Smith lag the estimates by 1 to 1.5 min. Their mean pitch angles are  $80^\circ$  and  $95^\circ$ , compared to  $\leq 50^\circ$  for the others, suggesting that this additional delay may be due to a weak dependence upon pitch angle.

[37] We conclude, therefore, that all the P1 pulses are consistent with the hypothesis that a cosmic ray pulse with temporal characteristics similar to that at high energies traveled from the vicinity of the Sun to Earth with  $\leq 1.5$  min delay due to scattering or dispersion other than velocity dispersion. Further, the characteristics of the asymptotic cones of acceptance, and the anisotropic P1 fluxes are such that Sanae and Climax only see high-energy cosmic rays with  $P > 3$  GV and  $\beta > 0.95$ . That is, the responses at Sanae and Climax were essentially free of velocity dispersion, and they therefore provide the most direct information about the near-Sun injection process.

[38] Using our modeled responses, we have also investigated the instantaneous nature of the cosmic ray spectrum throughout P1. Up to  $\sim 0653$  UT (i.e., near the peak), the spectrum above 3 GV approximated the original injection spectrum but was deficient in low-rigidity particles, i.e., it was a hard spectrum. By  $\sim 0657$  UT the high-rigidity component of P1 had declined; the low rigidities had reached their peak; the spectrum had softened markedly compared to the input spectrum, and the spectral exponent,  $\gamma$ , had increased by  $\geq 1$  unit. That is, there was a  $\sim 2$  min interval between the peak of P1 and the commencement of P2, when the spectrum arriving at Earth was anomalously soft as a consequence of velocity dispersion.

[39] In summary, the hypothesis that P1 was due to a short-lived release of cosmic rays (of all rigidities) into the HMF and propagation to Earth with little scattering finds support in (1) the differences between the several pulse shapes in Figure 6 being consistent with velocity dispersion of a single, short-lived pulse and (2) the strong anisotropy of P1 seen in Figure 8 and the small flux of radiation with pitch angles  $>90^\circ$ . The possibility that the intensity decrease at the end of the P1 event is merely due to the Earth moving from a flux tube of the HMF with little scattering to one with strong scattering is rendered unlikely by the time delays evident in Figure 6, but cannot be eliminated on the basis of this GLE alone. In section 6 we show, however, that the persistent observation of P1 events in the past, always at the beginning of a GLE, argues strongly against this possibility.

[40] On the basis of the  $\pi^0$ -pulse starting at  $\sim 0645:30$  UT and the type III radio burst at  $\sim 0646$  UT (Table 2), we have determined the transit time of the first arriving cosmic rays to be  $\sim 15$  min. This is demonstrated in Figure 10, which shows that there is good agreement between the onset phase of the  $\pi^0$ -pulse and the Sanae P1 pulse when the latter is moved backward in time by 7 min. Using equation (1), we have calculated that the mean rigidity at the 50% point on the rising phase of the pulse was 3.8 GV ( $\beta \approx 0.97$ ). Allowing  $\sim 1$  min for scattering implies a field-line length of  $1.76 \pm 0.1$  AU from the P1 injection point to Earth, compared to 1.08 AU for the Parker spiral field for a solar

**Table 3.** GLEs in the Archival Neutron Monitor Record That Exhibit Prompt, Highly Anisotropic Pulses, Similar to P1 Defined Herein, or Clearly Defined Worldwide Differences of Onset Time That May Indicate the Occurrence of an Undetected P1 Event<sup>a</sup>

Event	Date	Onset Difference (min)	Number of Stations With P1	Propagation Time Difference (min)	Position on Sun	Amplitude of P1/P2 (%)
1	7 Mar 1942	8	1	–	West Limb	4000/1500
2	23 Feb 1956	9	0	–1 (H <sub>α</sub> )	25°N, 85°W	?/ > 3000
3	4 May 1960	3	4	6 (H <sub>α</sub> )	10°N, 90°W	300/?
4	15 Nov 1960	30	2	11 (H <sub>α</sub> )	26°N, 35°W	160/80
5	7 May 1978	<5	10	9 (H <sub>α</sub> )	24°N, 68°W	215/–
6	29 Sep 1989	<5	3	17(X)	25°S, 98°W	250/200
7	22 Oct 1989	15	3	2(X)	27°S, 32°W	200/20
8	24 Oct 1989	14	0	–6(X)	29°S, 57°W	?/110
9	21 May 1990	10	2	11(X)	34°N, 37°W	20/5
10	24 May 1990	30?	2	11(X)	36°N, 76°W	50/7.5
11	15 Apr 2001	8	0	15(X)	20°S, 85°W	?/120
12	20 Jan 2005	8	4	4(X)	12°N, 58°W	2900/300
13	13 Dec 2006	10	6	10(X)	06°S, 24°W	100/20

<sup>a</sup>Column 2 gives the greatest difference in onset time, worldwide. The propagation time is estimated from the observed onset of a flare observed in H<sub>α</sub>, from ionospheric measurements, or from the occurrence of an intense microwave burst. It appears likely there was no P2 pulse in the 4 May 1960 GLE. (The 7 March 1942 event was only seen by ionization chambers, and the amplitudes given are the equivalent neutron monitor increases. This P1 event and the onset differences were recognized by K. G. McCracken when the original data recording films were examined in 2006.) The propagation time difference is the difference between the maximum of the solar activity (in H<sub>α</sub>, or X-ray and other emission) and the earliest cosmic ray increase. In the case of the 23 February 1956 event [Meyer *et al.*, 1956], a significant hesitation in the rising phase at Wellington is consistent with a P1 pulse.

wind speed of ~600 km/s observed by ACE. Figures 5 and 7 showed, however, that the HMF was highly inclined relative to the ecliptic, and this, together with the estimated transit time, suggests that the field line between Earth and the Sun throughout the P1 event extended to relatively high heliographic latitudes, resulting in this long path length.

## 6. Similar Events in the Past

[41] The salient features of the 20 January 2005 GLE are as follows: (1) for a few neutron monitors, an impulsive, highly anisotropic and intense cosmic ray pulse, consistent with a short-lived (~6 min) injection into the open HMF at the onset of the gamma ray burst due to the decay of  $\pi^0$ -mesons generated by the interaction of solar cosmic rays with coronal matter; (2) for several other neutron monitors, a much slower, mildly anisotropic event that commenced ~8 min after the first pulse; and (3) for a third group of neutron monitors a combination of the above. The H<sub>α</sub>, HXR and type III emissions of the parent flare peaked several minutes before the commencement of P1. We now consider the possibility that the worldwide cosmic ray network may have frequently failed to distinguish P1 from P2 in the past because of their rarity and little inter-station confirmation, with the occasional impulsive enhancement such as in Figure 1 being attributed to an ephemeral condition in the HMF.

[42] We have examined the historical record to identify GLEs that either show an impulsive enhancement similar to P1 at one or more cosmic ray detectors, or at least show a clearly defined difference in onset times between several high counting-rate neutron monitors. This study was restricted to the largest GLEs (>20% enhancements for at least one high-latitude neutron monitor) for which an isolated P1 event, such as seen by Sanae, will be statistically significant in 5 or 1 min data. For the 22 such >20% GLEs in the historical record (out of a total of 70), 13 meet the selection criteria and are listed in Table 3. Of the remaining 9 large GLEs that did not show these characteristics (and are classified as P2 events), four were due to solar activity near

the central solar meridian or on the eastern solar disk, and three were estimated to originate >15° behind the western limb of the Sun. Both classes will be discussed in the next paragraph. Note, in particular, that a P1 pulse has never been observed after the commencement of a P2 pulse in any of the 22 large GLEs examined. Ten out of the 13 GLEs in Table 3 exhibited short, impulsive enhancements similar to P1; the GLE of 22 October 1989 in Figure 1 being one of these. Column 4 shows that P1 pulses were usually seen by a small number of neutron monitors, while there have been more than 50 midlatitude and high-latitude neutron monitors in operation since 1957. The localized nature, the fast rise and fall times, and the short durations all indicate that the impulsive enhancements in all these cases were strongly anisotropic and similar to 20 January 2005. Column 3 shows that the delay between the first and last onset of a GLE was largely in the range 7 to 15 min, with an average of 12 min, broadly similar to the 8 min differences in onset given in Table 1 for 20 January 2005. Column 5 gives the difference between the earliest cosmic ray onset time, and the maxima of H<sub>α</sub>, radio or HXR emissions when available. The average “delay time” is 7.4 min, compared to ~4.5 min for 20 January 2005, consistent with the result that the P1 pulse is released into the open HMF coincident with, or soon after the most intense electromagnetic emissions from the flare. All these features indicate that many of the larger GLEs in the archival record exhibited characteristics similar to those of P1 and P2 in the event of 20 January 2005.

[43] Column 6 of Table 3 shows that all of the P1 events were observed in association with solar activity on the western portion of the solar disk (24° to 98°W). As noted above, seven of the large GLEs that did not exhibit a P1 pulse (or a large spread in onset times for P2) were either to the east of 24°W, or beyond 98°W. We interpret this as a geometric effect due to the HMF preventing the P1 population from reaching Earth. Figures 2 and 3 of Reames [1999] show that impulsive SEP events are associated with flares between 20° and 90°W, and this similarity provides strong support for the hypothesis that the P1 pulse of the GLE corresponds to the impulsive class of SEP events.

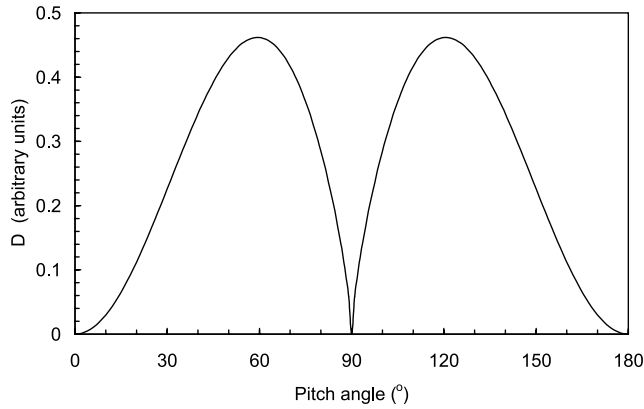


**Figure 12.** Dependence of the pitch angle diffusion coefficient  $D_{\mu\mu}$  upon pitch angle from (2), with  $q = 5/3$ .

Column 7 shows that the amplitude of the largest recorded P1 pulse was usually greater than that of the P2 pulse; in three cases it was 10 times greater. As discussed previously, the observed amplitude of the P1 pulse is critically dependent upon the alignment of the asymptotic cone with the anisotropy, and underestimation of the amplitude of P1 will always be likely. We therefore suggest that the maximum flux in the P1 pulse is usually a factor of  $\geq 10$  times that in the P2 pulse.

## 7. Discussion

### 7.1. Propagation of Pulses P1 and P2

[44] From the above, we conclude that the GLE of 20 January 2005 is a good representation of GLEs due to flares on the western portion of the solar disk. We propose that such events commonly consist of (1) a highly anisotropic, short-lived pulse, P1, due to cosmic rays that escape immediately into the open solar field soon after acceleration, that then travel unimpeded to Earth along the Parker field lines, and (2) a slowly rising and falling pulse, P2, that exhibits mild field-aligned anisotropies, and which starts 7 to 15 min after pulse P1. In most cases P1 has decayed to  $< 50\%$  of its maximum at one or two neutron monitors before P2 starts. In the following we outline a model to accommodate these features of the event of 20 January 2005, and the others in Table 3.

[45] The strong anisotropy of P1, its fast rise and fall, and its clearly defined velocity dispersion, all indicate that the scattering mean free path was  $> 1$  AU. In particular, the anisotropies in Figure 8 indicate that adiabatic focusing dominated over scattering, leading to this result. The absence of cosmic rays with pitch angles  $> 100^\circ$  indicates that there was no significant scattering in the immediate vicinity of Earth.

[46] Pulse P2 then appears to present a major contradiction, since its mildly anisotropic nature suggests a scattering mean free path  $< 0.5$  AU. Saiz *et al.* [2005] have proposed that the flow of electric current, in the form of the cosmic rays in pulse P1 contained sufficient energy to initiate magnetodynamic instabilities in the HMF. According to their model, those instabilities then strongly modified the scattering properties of the HMF, leading to a scattering

mean path of  $\sim 0.6$  AU when the P2 particles traversed it about 8 min later. Table 3 shows, however, that the amplitude of P1 for the GLE of 21 May 1990 was  $\sim 250$  times smaller than that of 20 January 2005. Consequently, the cosmic ray energy density for this small event was more than two orders smaller than that of the HMF, and insufficient to produce the effect proposed by Saiz *et al.* [2005].

[47] An alternative possibility is that the differing characteristics of P1 and P2 are the consequence of different degrees of scattering in adjacent regions of the HMF. For that model, the transition from P1 to P2 on 20 January 2005 would be a consequence of moving from a region of weak to strong scattering, due to the changes in the HMF (e.g., Figure 7). This scenario may be tenable for a single GLE; however, section 6 (Table 3) has shown that a P1 event has never occurred after the commencement of a P2 pulse in the 22 large GLEs in the historical record. Further, P2 events are typically ten times longer than P1. Consideration of these figures shows that the probability of P1 not occurring by chance after the commencement of P2 in this sample is  $< 10^{-4}$ . Thus, on the basis of the historical record, we discount this possibility.

[48] We have therefore sought another explanation for the major differences between the properties of P1 and P2. Small magnetic irregularities cause the first adiabatic invariant to be violated during a gyration about the large-scale field, leading to a small change in the pitch angle. Summing the effect over many gyrations results in pitch angle diffusion, quantified by the pitch angle diffusion coefficient  $D_{\mu\mu}$ . The strongest scattering effects are produced by the irregularities that are in resonance with the particle gyration. For the most commonly used treatment, namely the standard quasi-linear theory, the review of Dröge [2000] gives the pitch angle diffusion coefficient as

$$D_{\mu\mu}(\mu) = \frac{\pi(1 - \mu^2)\Omega^{2-q}v^{-q}\mu^{q-1}}{4B^2}, \quad (2)$$

where the cosmic ray gyrofrequency is  $\Omega$ , the cosine of the pitch angle is  $\mu$ ,  $v$  is particle speed, while the power spectrum at the resonant wave number of the transverse fluctuations in the HMF,  $B$ , is approximated by  $P_{\perp} = (\Omega/\mu v)^q$ . This shows that in the limiting case of a pitch angle near zero (or  $180^\circ$ ;  $\mu \approx \pm 1$ ), the  $(1 - \mu^2)$  term dominates; and  $D_{\mu\mu}(\pm 1) \approx 0$ . That is, cosmic rays with very small pitch angles are unaffected by the irregularities in the HMF. Cosmic rays injected into the HMF near the Sun with small pitch angles therefore suffer relatively little pitch angle diffusion, while experiencing adiabatic focusing that will largely counteract any scattering that does occur. Using  $q = 5/3$ ,  $D_{\mu\mu}(\mu)$  is plotted in Figure 12, which shows that it is a strong function of pitch angle. Thus, particles released with small pitch angles (or near  $180^\circ$ ) will suffer less scattering than those released with large pitch angles.

[49] In contrast to scattering, the process of adiabatic focusing in the background field reduces pitch angles due to the fact that  $\sin^2\theta/B$  is a constant of the motion. Since  $B \propto 1/r^2$  near the Sun, the nearer particles are released from the solar surface, the stronger they will be focused.

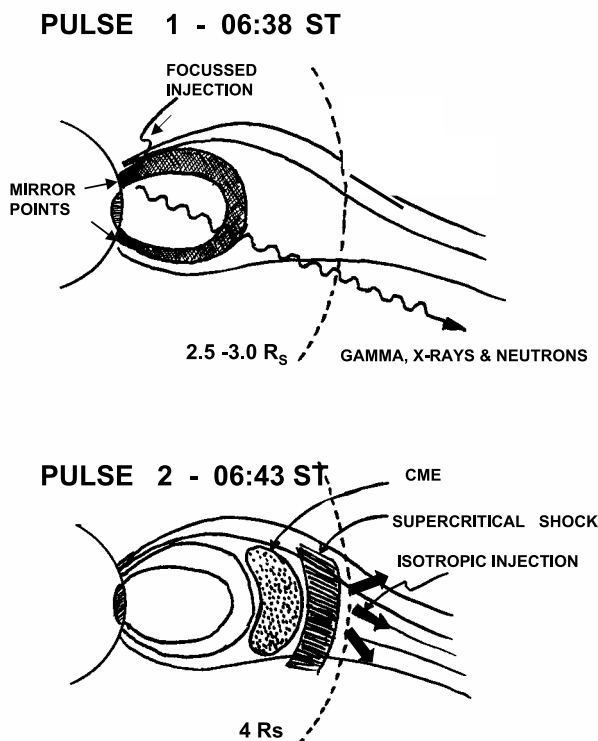


**Figure 13.** Schematic representation of the model proposed for the P1 and P2 pulses on 20 January 2005. (top) The situation at  $\sim 0638$  ST. The first accelerated population is trapped in the dark colored loop region adjacent to open magnetic field, and some of the solar cosmic rays are escaping immediately onto open field lines. They suffer little scattering but strong adiabatic focusing and arrive at Earth rapidly as the highly anisotropic pulse P1. The remainder of the solar cosmic rays from this acceleration episode are trapped in the sunspot magnetic fields. At the mirror points some collide with coronal atoms, emitting  $>90$  MeV  $\gamma$  rays. (bottom) The situation at or after  $\sim 0643$  ST, on a much enlarged scale. A coronal mass ejection launched by the flare has developed a strong supercritical shock. Cosmic rays accelerated in the shock are beginning to be injected into the HMF in a less anisotropic manner over a wide range of heliolongitudes. The majority suffer considerable pitch angle scattering, arriving at Earth as the slowly rising, mildly anisotropic pulse P2.

## 7.2. Source of the Particles in Pulses P1 and P2

[50] On the basis of the above discussion, we now advance a GLE model that consists of two separate populations of solar cosmic rays, as previously outlined by *McCracken and Moraal* [2007] and *Moraal et al.* [2007], and similar to those advanced by *Shea and Smart* [1998] and *Li and Zank* [2005] in respect of the lower-energy ( $<100$  MeV) SEP events. We take the view that any model of the GLE must benefit from, and be compatible with the model for the SEP events. As discussed in section 1, two distinct classes of SEP events are recognized: (1) impulsive events originating low in the corona and (2) gradual events occurring at a height of  $\sim 5$  solar radii in the outer corona.

The following discussion builds onto that existing model. Nevertheless, we note that the complexities of the solar environment and the static and dynamic characteristics of the HMF may mean that other models may be advanced in the future, either based on the observations herein or as a consequence of GLEs observed in the future.

[51] As discussed in section 5, the HXR and gamma ray data obtained by RHESSI and CORONAS-F, the concurrent observation of a strong type-III radio burst commencing at  $>300$  MHz; and the velocity dispersion and anisotropy of the P1 pulse at Earth have led us to suggest that the P1 population was accelerated in the lower corona, and a portion of the population was released immediately into the open magnetic field at  $\sim 0638$  ST (Figure 13). As mentioned above, the field strength of the coronal magnetic field decreases rapidly with radial distance, and we therefore propose that adiabatic focusing along the open field lines resulted in pitch angles of, say,  $<10^\circ$  by the time these particles had reached  $2.5 R_s$ , the conventional lower boundary of the HMF. Thus these P1 particles would then propagate to Earth from this point onward with little scattering (see Figure 12), while experiencing further adiabatic focusing, resulting in the highly anisotropic, velocity dispersed P1 pulse at Earth. As discussed previously, only a few neutron monitors would observe such a narrowly focused pulse.

[52] In section 5 we estimated that pulse P1 took 15 min to travel a distance of  $1.76 \pm 0.1$  AU to Earth. This sets an upper limit for the P2 propagation time; depending on the angular extent of the CME, as discussed in the next paragraph. Pulse P2 commenced at Earth at  $\sim 0658$  UT, and a propagation time of  $\leq 15$  min indicates that the P2 particles started to leave the Sun at or after 0643 ST. Unlike P1, there was no synchronous enhancement in the high-energy gamma ray emissions (i.e., no increase observed at Earth at  $\sim 0652$  UT), showing that the P2 population had no direct magnetic connection to the higher densities in the lower corona.

[53] *Simnett and Roelof* [2005] used the RHESSI data to estimate that the CME associated with the flare of 20 January 2005 lifted off at 0632 ST, and was traveling with a sky plane speed of  $\sim 2500$  km/s, while *Gopalswamy et al.* [2005] give a speed of 3675 km/s. In a detailed analysis, *Grechnev et al.* [2008] concluded that the sky plane speed was in the range 2000–2600 km/s, and that the CME was at  $4.4 R_s$  at 0646 ST. On the basis of these estimates, and the estimated P2 departure time at or after 0643 ST, the leading edge of the CME would have been at or above the range  $3.3$ – $3.8 R_s$  when the first P2 particles departed for Earth. *Mann et al.* [2003] have shown that the Alfvén velocity,  $V_A$ , drops from  $>1000$  km/s in the vicinity of a large sunspot group to a minimum of  $\sim 200$  km/s, in some circumstances, at  $1.5 R_s$ . It then increases steadily to  $\sim 700$  km/s, and then falls off steadily again for increasing distance from the Sun. For a CME velocity  $\sim 2500$ – $3500$  km/s, the Alfvén Mach number would have been  $\geq 5$ , and efficient acceleration of ions would occur in a shock developing in this region.

[54] On the basis of all the GLEs observed during solar cycle 23, and the concurrent images of the corona made by the SOHO spacecraft, *Gopalswamy et al.* [2005] have shown that GLEs are always associated with a coronal mass ejection (CME). They only used the data from one neutron

monitor (Oulu), and consequently their result refers primarily to the P2 pulse. They further concluded that the CMEs associated with GLEs have higher mean velocities than those associated with SEP events. In agreement with an earlier study by *Kahler* [1994], they concluded that the GLE particles were injected into the HMF at an average height of  $\sim 4.5$  solar radii. These results are all consistent with our study of the P2 pulse, and we proceed on the basis that it originated in a shock wave associated with the CME observed following the flare of 20 January 2005.

[55] Pulse P1 has shown that there was a good magnetic connection from the Sun to Earth. On the basis of the discussion in section 7.1, the mild anisotropy of P2 is then explicable in terms of the P2 particles being injected into the HMF from the front of the CME in an approximately isotropic manner (consistent with diffusive shock acceleration) so that the majority of the particles suffered substantial pitch angle scattering en route to Earth. The delay times in column 5 of Table 3, and the mild anisotropies are consistent with the P2 pulse being emitted into the open magnetic field in the range  $3 < R_s < 5$  in all the GLEs listed in Table 3.

[56] Section 6 showed that the P2 pulse was observed over a solar longitude range of  $\sim 140^\circ$ , compared to  $\sim 70^\circ$  for P1. CMEs are observed to extend to solar longitudes  $> 45^\circ$  on either side of their origin, and acceleration of a P2 population in an associated shock wave may consequently result in the P2 GLE being observed over a wider range of longitudes than P1. For a GLE such as that of 20 January 2005, this suggests that the particles in the P2 pulse may have been injected into the HMF by the CME over the longitude range  $15^\circ$ – $105^\circ$ W, and up to solar latitudes of  $\sim 45^\circ$ . That is, the P2 cosmic ray source would be well distributed in solar longitude, while the P1 source, being in close proximity of the parent sunspot and low in the corona, would be considerably more localized. One consequence of this is that the first of the P2 cosmic rays to reach Earth may have left the Sun well removed from the P1 injection point, and may have traveled a lesser distance to Earth than the P1 pulse as suggested above.

[57] In summary, the observations of 20 January 2005 and the others in Table 3 are consistent with a model wherein particle acceleration occurred in two different regions of the corona, as summarized in Figure 13. In that model, ions and electrons were first accelerated to relativistic energies at  $\sim 0638$  ST and trapped in the closed magnetic fields of the sunspot group. They generated bremsstrahlung, knock-on neutrons, and  $\pi^0$ -mesons at their mirror points at low coronal altitudes. For a short time immediately after the acceleration episode, a portion of the newly accelerated cosmic rays and electrons escaped onto open field lines low in the corona [e.g., *Reames*, 2002] and adiabatic focusing in the corona meant that they were injected into the HMF with low pitch angles, and consequently reached Earth rapidly as a short-lived, highly anisotropic, velocity dispersed pulse. We associate this initial pulse with the “impulsive” SEP event often seen at lower particle energies.

[58] The remainder of the P1 population remained trapped in the sunspot magnetic fields, leading to a slowly declining flux of  $> 90$  MeV gamma rays. A shock developed ahead of the associated CME at or after  $\sim 0642$  ST, and commenced to accelerate relativistic particles. The P2 population then started to escape ahead of the shock into

the HMF in a relatively isotropic manner, over an extended range of longitudes, and as outlined above, suffered pitch angle diffusion to reach Earth in a slowly rising, mildly anisotropic pulse of radiation.

[59] The above model for the composite GLE is consistent with the mixed particle acceleration model proposed by *Li and Zank* [2005] for SEP events. The “gradual” class of SEP events is attributed to acceleration in the shock ahead of a CME; *Kahler* [1994] has shown that the energetic particles leave the vicinity of the Sun when the CME reaches  $\geq 4$  solar radii. We therefore propose that the P2 pulses in the event of 20 January 2005 and in the other GLEs in Table 3 were the relativistic manifestation of the gradual SEP events.

### 7.3. Generic GLE

[60] There is a longstanding working model wherein the characteristics of the GLE observed at Earth are determined by (1) the position of the parent solar activity on the solar disk, (2) the initial large- and small-scale configuration of that field, and (3) the time-dependent configuration of the HMF, both inside and outside the orbit of Earth. It is also well accepted that there are two classes of SEP events observed at low energies, the impulsive and the gradual ones. On the basis of the forgoing sections, we now propose a revised working model for the GLE, which accommodates, in particular, the P1 and P2 pulses discussed herein. Following that, we briefly discuss the influence of the HMF on the composite GLE observed near the orbit of Earth.

[61] We propose that the generic GLE consists of two separate populations of solar cosmic rays, as does the generic model of the SEP events at low energies. The first population, responsible for the P1 pulse, escapes onto open field lines of the HMF immediately after a short-lived ( $\sim 6$  min) acceleration episode in the vicinity of a large solar flare. The acceleration is approximately synchronous with the emission of HXR and gamma rays by the flare. The acceleration and escape into the open HMF occurs in the low corona. This population has a hard source spectrum. A portion of the newly accelerated cosmic radiation remains trapped in the sunspot magnetic fields. It is suggested that this part of the GLE corresponds to the “impulsive” solar energetic particle (SEP) event at lower energies.

[62] We further propose that the second component of the generic GLE is responsible for the P2 pulse. The source spectrum is softer, and the cosmic rays escape into the HMF in the vicinity of 3–5 solar radii some 8–15 min after the release of the P1 population. It appears likely that this population has been accelerated in a shock wave driven by the CME associated with the parent flare. We associate this portion of the GLE with the “gradual” SEP event at lower energies.

[63] Following release, the HMF may strongly modify the characteristics of both populations, as seen at Earth. Thus it has been long recognized that the location of a flare on the solar disk will strongly influence the propagation conditions between Sun and Earth. The historical record shows that the P1 population gains access to Earth if the parent flare occurs between  $\sim 24^\circ$  and  $98^\circ$ W on the solar disk, attributable to the spiral nature of the open field. The P2 population reaches Earth after solar activity in the range  $\sim 45^\circ$ E to  $130^\circ$ W, attributable to release into the HMF from

a shock wave expanding rapidly over  $\sim 90$  degrees of longitude centered on the parent solar activity.

[64] The occurrence of a Forbush decrease several days prior to a GLE has a substantial influence on the characteristics of a GLE. The HMF has a major effect upon the detailed nature of the anisotropies of both components of the generic GLE as discussed in section 7.2. Some GLEs (both P1 and P2) exhibit anisotropies that are persistent from the direction to the Sun, while others exhibit anisotropies from the sunward and anti-Sun directions at different times during the GLE. Some GLEs exhibit variations attributable to time-dependent changes in the direction of the HMF as in the case of the P3 event on 20 January 2005. In other cases a CME sweeps past the Earth, carrying fluxes of trapped cosmic rays, and modifying the cutoff rigidities and asymptotic cones of the worldwide network of neutron monitors (e.g., 12 November 1960, an extreme case where a major unassociated Forbush decrease commenced  $\sim 1$  h after the commencement of the GLE). Clearly, the detailed nature of the GLE will vary in a substantial manner from one to another. However, the frequent occurrence of the P1 pulse ahead of a P2 pulse in the large events in Table 3 indicates that this is an important feature of the GLE that is not erased by scattering or time variability in the HMF.

## 8. Conclusions

[65] We have shown that the GLE of 20 January 2005 is consistent with the arrival at Earth as two separate pulses of cosmic radiation. The first pulse, P1, was fast-rising, short-lived, field-aligned, and highly anisotropic. It was only seen by neutron monitors whose asymptotic cones of acceptance were directed to the vicinity of  $85^\circ\text{S}$ ,  $40^\circ\text{W}$  (geographic). The  $>3$  GV particles in it arrived at Earth at  $\sim 0650$  UT, the intensity peaked at  $\sim 0653$  UT, and the pulse had decreased to 50% of its maximum by  $\sim 0656$  UT.

[66] The second pulse (P2) was also field-aligned, and commenced 7 to 8 min after the start of P1 as a mildly anisotropic, slowly rising pulse, similar to the “typical” GLE. It exhibited a softer spectrum than P1. It was seen widely throughout the world, and remained field-aligned for the subsequent hour. The observation of a third pulse by some neutron monitors viewing in asymptotic directions in the range  $30^\circ$ – $100^\circ\text{E}$  was due to the rotation of the P2 anisotropy in space due to the changing direction of the HMF.

[67] The first cosmic ray pulse (P1) was highly anisotropic with a Gaussian characteristic angle of  $50^\circ$ . Comparison with GLEs in 1960, 1978 and 1989 shows a remarkable similarity between the pitch angle dependence of these events at different phases of the solar cycle, suggesting that this is a consistent feature of the P1 pulse.

[68] The RHESSI observations show that the X-ray emissions associated with the flare developed a loop-like structure at 0639 UT. Two regions of intense emission of hard X rays then appeared  $\sim 7^\circ$  to the east of the initial X-ray emissions associated with the solar flare. A strong pulse of  $>90$  MeV gamma rays, from  $\pi^0$ -decay, was observed by the CORONAS-F satellite, starting at 0645:20 UT, indicating that a population of relativistic cosmic rays started to develop at 0637:10 ST. The gamma ray emissions and the localized HXR emissions persisted for  $>10$  min, which we attribute to

trapping of solar electrons and cosmic rays in the closed magnetic fields of the sunspot group.

[69] We have shown that the properties of the P1 pulse are explicable in terms of a  $\sim 6$  min release of relativistic cosmic rays into the HMF starting at 0637:10 ST. It showed clearly defined velocity dispersion, consistent with  $<1.5$  min delay due to diffusive effects en route to Earth. This, and the highly anisotropic nature of the pulse indicates that there was little diffusive scattering en route from the Sun. Comparison of the cosmic ray and  $>90$  MeV gamma ray pulses yields a transit time of  $\sim 15$  min for the P1 pulse. Our analysis predicts that the velocity dispersion results in the cosmic ray spectrum exhibiting an anomalously soft rigidity spectrum ( $\gamma \approx -9$ ) for several minutes between the P1 and P2 pulses.

[70] Examination of the 22 largest GLEs in the historical record since 1942 has shown that short, impulsive enhancements similar to P1, or onset differences indicative of them, have preceded 13 of the 15 GLE that originated between  $24^\circ\text{W}$  and  $98^\circ\text{W}$  on the solar disk. The time durations were similar and they were all highly anisotropic. This leads us to propose that the presence of the two pulses, P1 and P2, is a common feature of all GLEs. Several examples suggest that the P1 pulse may exhibit fluxes  $\geq 10$  times those in the P2 pulse. The historical record shows that GLEs corresponding to solar activity outside the range  $\sim 24^\circ$  to  $115^\circ\text{W}$  exhibited P2 events only.

[71] In particular, the historical record shows that P1 events always precede P2 events. This is a vital observation, and shows that occurrence of a P1 pulse followed by P2 cannot be due to the Earth moving by chance from a HMF flux tube with little scattering, to one with strong scattering.

[72] At first sight, the greatly different time profiles and anisotropic natures of P1 and P2 appear to be incompatible. However, following *Dröge* [2000], we note that pitch angle diffusion is a strong function of pitch angle, and that the characteristics of P1 are explicable if the particles were injected into the HMF with pitch angles  $<10^\circ$ . Much more isotropic injection of the P2 population would lead to slow rise and fall times, as well as the mild anisotropies observed by the neutron monitor network.

[73] The starting time of the P2 pulse at Earth indicates that the P2 population first left the Sun at or later than  $\sim 0642:30$  ST. On the basis of the work of *Mann et al.* [2003] we propose that the CME initiated by the solar flare drove a super-critical magnetohydrodynamic shock that accelerated cosmic rays when it was in the vicinity of, or above 3.3–3.8 solar radii. We propose that these cosmic rays were injected into the HMF with a more isotropic pitch angle distribution, and over a wide range of longitudes as a consequence of the breadth of the CME. The majority of the P2 population then suffered substantial diffusion en route to Earth to arrive at Earth as the slowly rising, mildly anisotropic P2 pulse. Previous work, as well as our analysis, indicates that the source spectrum of P1 was harder than that of P2.

[74] We have proposed a “generic GLE,” comprising the two separate cosmic ray populations, P1, and P2. P1, with its hard spectrum is injected into the open field low in the corona as a short-lived ( $\sim 6$  min) pulse at the time of the HXR, gamma rays, knock-on neutrons, and Type III radio emissions. P2, with its softer spectrum is injected into the



open field some 8 to 15 min later when the CME associated with the flare is in the vicinity of 3 to 5 solar radii. The prevailing configuration of the HMF, both inside and outside the orbit of Earth, modifies the characteristics of both P1 and P2 when they arrive at Earth.

[75] The observations of the GLE of 20 January 2005, as well as earlier ones, have led us to propose that pulses P1 and P2 of the GLE are the relativistic manifestations of the “impulsive” and “gradual” events seen in SEP events at lower energies.

[76] **Acknowledgments.** The operation of the Sanae neutron monitor was supported by the South African National Antarctic Programme (SANAP). NSF grant ATM0107181 supported the work at the University of Maryland. We thank J. W. Bieber and the Bartol Research Institute for provision of the neutron monitor data from “Spaceship Earth.” Neutron monitors of the Bartol Research Institute are supported by NSF grant ATM-0527878. We also acknowledge the important contributions made to this paper by the neutron monitors operated by the Australian Antarctic Division, and the University of New Hampshire. We acknowledge with thanks the unpublished CORONAS-F gamma ray data supplied by V. G. Kurt and the asymptotic directions provided by M. L. Duldig and D. J. Bombardieri. Finally, we acknowledge the hospitality of the Carnegie Institution of Washington and the assistance of Shaun Hardy to retrieve the Forbush ionization chamber data of the 1940s.

[77] Zuyin Pu thanks the reviewers for their assistance in evaluating this paper.

## References

- Bieber, J. W., W. Dröge, P. A. Evenson, K. R. Pyle, D. Ruffolo, U. Pinsook, P. Toopraka, M. Rujiwarodom, T. Khumlumert, and S. Krucker (2002), Energetic particle observations during the 2000 July 14 solar event, *Astrophys. J.*, *567*, 622–634, doi:10.1086/338246.
- Bieber, J. W., J. Clem, P. A. Evenson, K. R. Pyle, M. Duldig, J. E. Humble, D. Ruffolo, M. Rujiwarodom, and A. Saiz (2005), Largest GLE in half a century: Neutron monitor observations of the January 20, 2005 event, in *Proceedings of the 29th International Cosmic Ray Conference*, vol. 1, pp. 237–240, Tata Inst. of Fundam. Res., Mumbai, India.
- Bombardieri, D. J. (2008), Modelling cosmic ray ground level enhancements and relativistic solar proton acceleration, Ph.D. thesis, Univ. of Tasmania, Hobart, Australia.
- Bombardieri, D. J., M. L. Duldig, K. J. Michael, and J. E. Humble (2006), Relativistic proton production during the 14 July 2000 solar event: The case for multiple source mechanisms, *Astrophys. J.*, *644*, 565–574, doi:10.1086/501519.
- Clem, J. M., and L. I. Dorman (2000), Neutron monitor response functions, *Space Sci. Rev.*, *93*, 335–359, doi:10.1023/A:1026508915269.
- Cramp, J. L., M. L. Duldig, E. O. Flueckiger, J. E. Humble, M. A. Shea, and D. F. Smart (1997), The October 22, 1989, solar cosmic ray enhancement: An analysis of the anisotropy and spectral characteristics, *J. Geophys. Res.*, *102*, 24,237–24,248, doi:10.1029/97JA01947.
- D’Andrea, C., and J. Poirier (2005), Ground level muons coincident with the 20 January 2005 solar flare, *Geophys. Res. Lett.*, *32*, L14102, doi:10.1029/2005GL023336.
- Dröge, W. (2000), Particle scattering by magnetic fields, *Space Sci. Rev.*, *93*, 121–151, doi:10.1023/A:1026588210726.
- Firor, J. (1954), Cosmic ray time variations, 4. Increases associated with solar flares, *Phys. Rev.*, *94*, 1017–1028, doi:10.1103/PhysRev.94.1017.
- Flueckiger, E. O., R. Butikofer, M. R. Moser, and L. Desorgher (2005), The cosmic ray ground level enhancement during the Forbush decrease in January, 2005, in *Proceedings of the 29th International Cosmic Ray Conference*, vol. 1, pp. 225–229, Tata Inst. of Fundam. Res., Mumbai, India.
- Forbush, S. E. (1946), Three unusual cosmic-ray increases possibly due to charged particles from the Sun, *Phys. Rev.*, *70*, 771–772, doi:10.1103/PhysRev.70.771.
- Gopalswamy, N., H. Xie, S. Yashiro, and I. Usoskin (2005), Coronal mass ejections and ground level enhancements, in *Proceedings of the 29th International Cosmic Ray Conference*, vol. 1, pp. 169–172, Tata Inst. of Fundam. Res., Mumbai, India.
- Grechnev, V. V., et al. (2008), The extreme solar event of 20 January 2005: Properties of the flare and origin of energetic particles, *Sol. Phys.*, *252*, 149–177, doi:10.1007/s11207-008-9245-1.
- Kahler, S. (1994), Injection profiles of solar energetic particle as function of coronal mass ejection heights, *Astrophys. J.*, *428*, 837–842, doi:10.1086/174292.
- Kuznetsov, S. N., V. G. Kurt, B. Y. Yushkov, and K. Kudela (2007), CORONAS-F satellite data on the delay between the proton acceleration on the sun and their detection at 1 AU, paper presented at 30th International Cosmic Ray Conference, Univ. Nac. Autónoma de México, Merida, Mexico.
- Li, G., and G. P. Zank (2005), Mixed particle acceleration at CME-driven shocks and flares, *Geophys. Res. Lett.*, *32*, L02101, doi:10.1029/2004GL021250.
- Lovell, J. L., M. L. Duldig, and J. E. Humble (1998), An extended analysis of the September 1989 cosmic ray ground level enhancement, *J. Geophys. Res.*, *103*, 23,733–23,742, doi:10.1029/98JA02100.
- Mann, G., A. Klassen, H. Aurass, and H. T. Classen (2003), Formation and development of shock waves in the solar corona and the near-Sun interplanetary space, *Astron. Astrophys.*, *400*, 329–336, doi:10.1051/0004-6361:20021593.
- McCracken, K. G. (1962a), The cosmic-ray flare effect: 1. Some new methods of analysis, *J. Geophys. Res.*, *67*, 423–434, doi:10.1029/JZ067i002p00423.
- McCracken, K. G. (1962b), The cosmic-ray flare effect: 2. The flare effects of May 4, November 12, and November 15, 1960, *J. Geophys. Res.*, *67*, 435–446, doi:10.1029/JZ067i002p00435.
- McCracken, K. G., and H. Moraal (2007), Two acceleration mechanisms for the 20 January 2005 ground level enhancement, paper presented at 30th International Cosmic Ray Conference, Univ. Nac. Autónoma de México, Merida, Mexico.
- McCracken, K. G., and R. A. R. Palmeira (1960), Comparison of cosmic-ray injections, *J. Geophys. Res.*, *65*, 2673–2683, doi:10.1029/JZ065i009p02673.
- Meyer, P., E. N. Parker, and J. A. Simpson (1956), Solar cosmic rays of February 23, 1956 and their propagation through interplanetary space, *Phys. Rev.*, *104*, 768–783, doi:10.1103/PhysRev.104.768.
- Miroshnichenko, L. I., K.-L. Klein, G. Trotter, P. Lantos, E. V. Vashenyuk, Y. V. Balabin, and B. B. Gvozdevsky (2005), Relativistic nucleon and electron production in the 2003 October 28 solar event, *J. Geophys. Res.*, *110*, A09S08, doi:10.1029/2004JA010936.
- Miyasaka, H., et al. (2005), The solar event on 20 January 2005 observed with the Tibet YBJ neutron monitor observatory, in *Proceedings of the 29th International Cosmic Ray Conference*, vol. 1, pp. 241–244, Tata Inst. of Fundam. Res., Mumbai, India.
- Moraal, H., K. G. McCracken, and P. H. Stoker (2007), Analysis of the 20 January 2005 ground level enhancement, paper presented at 30th International Cosmic Ray Conference, Univ. Nac. Autónoma de México, Merida, Mexico.
- Parker, E. N. (1958), Dynamics of the interplanetary gas and magnetic fields, *Astrophys. J.*, *128*, 664–676, doi:10.1086/146579.
- Plainaki, C., A. Belov, E. Eroshenko, H. Mavromichalaki, and V. Yanke (2007), Modeling ground level enhancements: Event of 20 January 2005, *J. Geophys. Res.*, *112*, A04102, doi:10.1029/2006JA011926.
- Reames, D. V. (1999), Particle acceleration at the Sun and in the heliosphere, *Space Sci. Rev.*, *90*, 413–491, doi:10.1023/A:1005105831781.
- Reames, D. V. (2002), Magnetic topology of impulsive and gradual solar particle events, *Astrophys. J.*, *571*, L63–L66, doi:10.1086/341149.
- Ryan, J. M., and the Milagro Consortium (2005), Ground-level events measured with Milagro, in *Proceedings of the 29th International Cosmic Ray Conference*, vol. 1, pp. 245–248, Tata Inst. of Fundam. Res., Mumbai, India.
- Saiz, A., D. Ruffolo, M. Rujiwarodom, J. W. Bieber, J. Clem, P. A. Evenson, R. Pyle, M. L. Duldig, and J. E. Humble (2005), Relativistic particle injection and interplanetary transport during the January 20, 2005 ground level enhancement, in *Proceedings of the 29th International Cosmic Ray Conference*, vol. 1, pp. 229–232, Tata Inst. of Fundam. Res., Mumbai, India.
- Shea, M. A., and D. F. Smart (1982), Possible evidence for a rigidity-dependent release of relativistic protons from the solar corona, *Space Sci. Rev.*, *32*, 251–257.
- Shea, M. A., and D. F. Smart (1996), Unusual intensity-time profiles of ground-level solar proton events, in *High Energy Solar Physics*, edited by R. Ramaty, N. Mandzhavidze, and X.-M. Hua, *AIP Conf. Proc.*, *374*, 131–139.
- Shea, M. A., and D. F. Smart (1998), Relativistic solar proton events—Evidence for a dual-state injection scenario, in *Advances in Solar Connection With Transient Interplanetary Phenomena*, edited by F. Xueshang, W. Fengsi, and M. Dryer, pp. 467–474, Int. Acad., Beijing.
- Simnett, G. M., and E. C. Roelof (2005), Timing of the relativistic proton acceleration responsible for the GLE on 20 January 2005, in *Proceedings of the 29th International Cosmic Ray Conference*, vol. 1, pp. 233–236, Tata Inst. of Fundam. Res., Mumbai, India.
- Stoker, P. H. (1994), Relativistic solar proton events, *Space Sci. Rev.*, *73*, 372–385.

Stoker, P. H., L. I. Dorman, and J. Clem (2000), Neutron monitor design improvements, *Space Sci. Rev.*, *93*, 361–380, doi:10.1023/A:1026560932107.

Tsyganenko, N. A. (1989), A magnetospheric magnetic field model with a warped tail current sheet, *Planet. Space Sci.*, *37*, 5–20, doi:10.1016/0032-0633(89)90066-4.

H. Moraal and P. H. Stoker, School of Physical and Chemical Sciences, North-West University, Potchefstroom 2520, South Africa. (harm.moraal@nwu.ac.za; pieter.stoker@nwu.ac.za)

---

K. G. McCracken, Institute for Physical Science and Technology, University of Maryland, College Park, MD 20742, USA. (jellore@hinet.net.au)